

NUREG/CR-1946
LA-8702-MS



Slab Core Test Facility
Steam Supply Design Analysis with TRAC

120555064215 2 ANR4
US NRC
ACM DOCUMENT CONTROL DESK
PDR
016
WASHINGTON DC 20555

University of California



LOS ALAMOS SCIENTIFIC LABORATORY

Post Office Box 1663 Los Alamos, New Mexico 87545

B107060053 B10630
PDR NUREG
CR-1946 R PDR

An Affirmative Action/Equal Opportunity Employer

NOTICE

This report was prepared as an account of work sponsored by an agency of the United States Government. Neither the United States Government nor any agency thereof, or any of their employees, makes any warranty, expressed or implied, or assumes any legal liability or responsibility for any third party's use, or the results of such use, of any information, apparatus, product or process disclosed in this report, or represents that its use by such third party would not infringe privately owned rights.

Slab Core Test Facility Steam Supply Design Analysis with TRAC

Suzanne T. Smith

Manuscript submitted: January 1981

Date published: May 1981

Prepared for
Division of Reactor Safety Research
Office of Nuclear Regulatory Research
US Nuclear Regulatory Commission
Washington, DC 20555

NRC FIN No. A7049



SLAB CORE TEST FACILITY STEAM SUPPLY DESIGN ANALYSIS WITH TRAC

by

Suzanne T. Smith

ABSTRACT

Early TRAC calculations for the Slab Core Test Facility indicated an external source of steam may be necessary to achieve refill and reflood behavior typical of a full-scale pressurized water reactor during a postulated loss-of-coolant accident sequence. To resolve this issue, a series of parametric calculations has been performed, using as a basis a set of five combinations of upper plenum and cold-leg emergency core coolant water temperatures. These cases were then run with ten parametric variations. The conclusion from this study is that the external steam source is unnecessary, but its inclusion would lend flexibility for future tests.

I. INTRODUCTION

The 2D-3D Program is a multinational analysis and experimental program to study detailed multidimensional behavior of the major subsystems of a nuclear power plant during a postulated loss-of-coolant accident (LOCA) sequence. The Federal Republic of Germany has built and is operating the Primary Coolant Loop Test Facility (PKL) and will build and operate the Upper Plenum Test Facility (UPTF). The Japan Atomic Energy Research Institute (JAERI) has built and is operating two of the test facilities: the Cylindrical Core Test Facility (CCTF), a full-height, one-fifth radial scale electrically heated facility, and the Slab Core Test Facility (SCTF), a full-height, eight-bundle-wide

electrically heated slab facility. The Los Alamos National Laboratory, through support of the United States Nuclear Regulatory Commission (USNRC), is responsible for the analysis support and for some of the instrumentation design and fabrication.

The analysis tool used is the Transient Reactor Analysis Code (TRAC)¹ being developed at the Los Alamos National Laboratory to provide an advanced "best estimate" predictive capability for the analysis of postulated accidents in light water reactors. TRAC provides this analysis capability for pressurized water reactors (PWRs) and for a wide variety of thermal-hydraulic experimental facilities. It features a three-dimensional treatment of the pressure vessel and associated internals, one-dimensional loop component models, two-phase nonequilibrium hydrodynamics models, flow-regime-dependent constitutive equation treatment, reflood tracking capability for both bottom flood and falling film quench fronts, and consistent treatment of entire accident sequences including the generation of consistent initial conditions.

The purpose of the SCTF experiments is to provide insight into the thermal-hydraulic behavior of a PWR during the end-of-blowdown, refill and reflood phases of a hypothetical loss-of-coolant accident sequence. Of particular interest are core radial flow distributions, liquid entrainment in the core and carryover into the upper plenum, upper plenum liquid pool formation and fallback into the core, quench front propagation, condensation effects, emergency core cooling performance, and overall refill and reflood behavior.

The SCTF designers intended the slab to simulate a radial slice of a typical PWR from its center through the vessel wall. The typical PWR is intended to be either the 15 x 15 Westinghouse/Japanese reference PWR or the 16 x 16 German PWR. The SCTF Core I design is a compromise between these two reference PWRs; the number of spacers and axial lengths will simulate the Westinghouse/Japanese reactor, whereas the horizontal width will represent the Kraftwerk Union (KWU) German PWR design.

The facility is composed of the pressure vessel, primary coolant system, emergency core cooling (ECC) system, and two containment tanks. The pressure vessel contains the core, downcomer, upper and lower plena, barrel baffle region, and upper head. The primary coolant system comprises an intact loop, a broken loop with valves to simulate breaks, a steam-water separator, and a pump simulator. ECC water can be injected into the cold leg between the vessel and the steam-water separator and through four injection ports directly into the upper plenum above the tie-plate.

A much-debated issue in the design of the SCTF has been whether or not to include an external steam supply. Based on early* TRAC calculations,² it appeared that an added source of steam was necessary to achieve end-of-blowdown core steam flow rates calculated for the refill phase of an accident recovery sequence for a postulated LOCA in a German pressurized water reactor (GPWR). Because of a concern that the enhanced steam flows might damage the facility or the instrumentation, the USNRC thought that further TRAC analysis should be used to resolve the issue.

A later series of calculations³ was then performed using both a finer vessel noding scheme axially and radially and a slightly later version of the early TRAC code. Three time-dependent steam supplies were considered, and four different injection locations were tried. It was concluded from this previous set of calculations that none of the steam supplies tried thus far had significantly improved on the base case (no extra steam) in approximating GPWR end-of-blowdown conditions.

*That series of calculations used a vessel noding scheme encompassing two bundles for each radial node. It also used an early (pre-PIA) version of TRAC. The results indicated that steam flow rates through the core were in the negative direction.

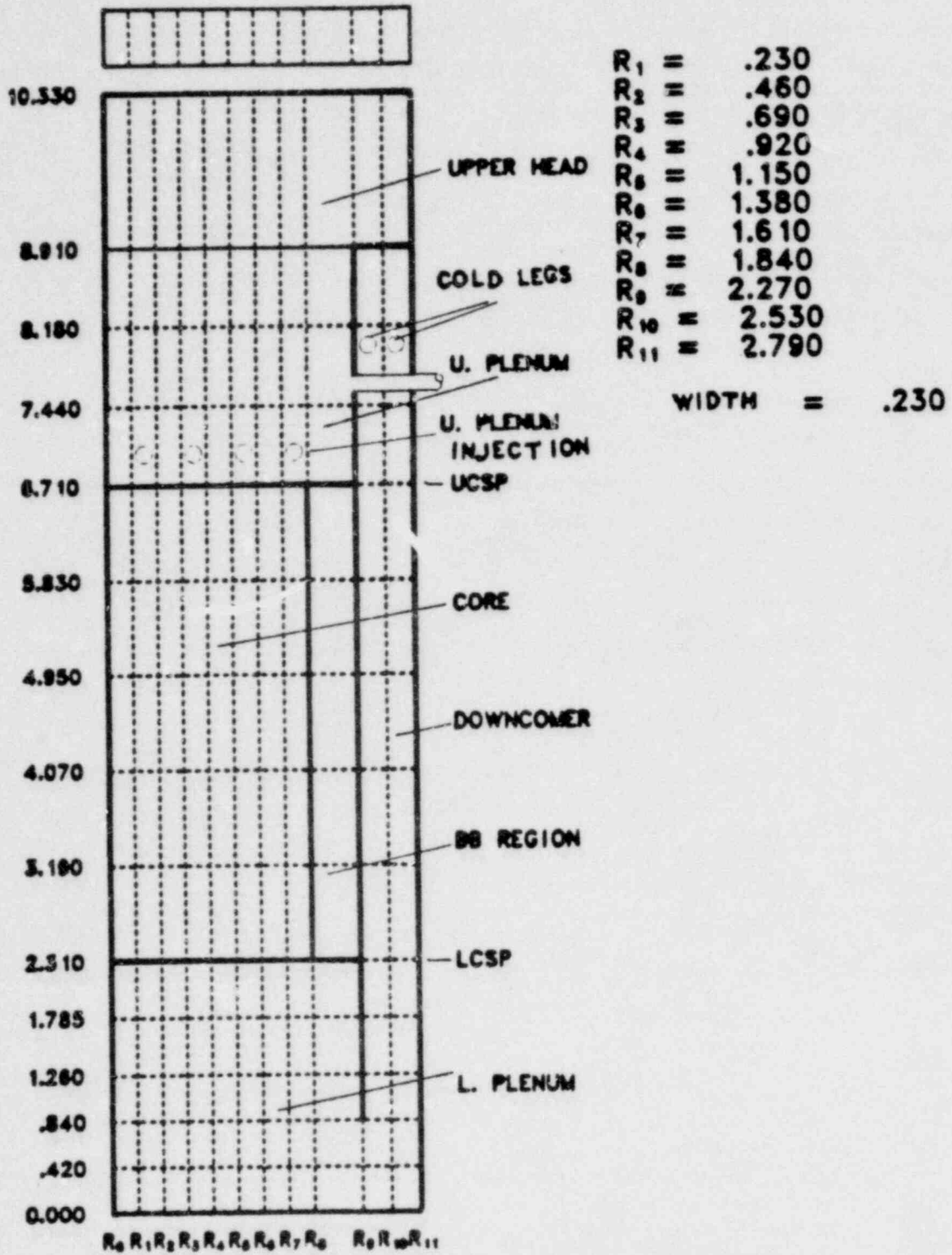


Fig. 1. SCTF vessel noding diagram.

II. THE CURRENT STUDY

Another series of calculations⁴ was requested by JAERI in which a 1 kg/s steam supply, uniformly distributed radially across the core width in eight pipes (one per bundle), was injected upward from the bottom of the lower plenum. Figure 1 is the vessel noding diagram. The system component diagram is shown in Fig. 2. JAERI proposed a set of four cases differing from one another in the temperatures of the cold-leg and upper plenum ECC water and in the inclusion of the external steam source. A logical extension was a fifth

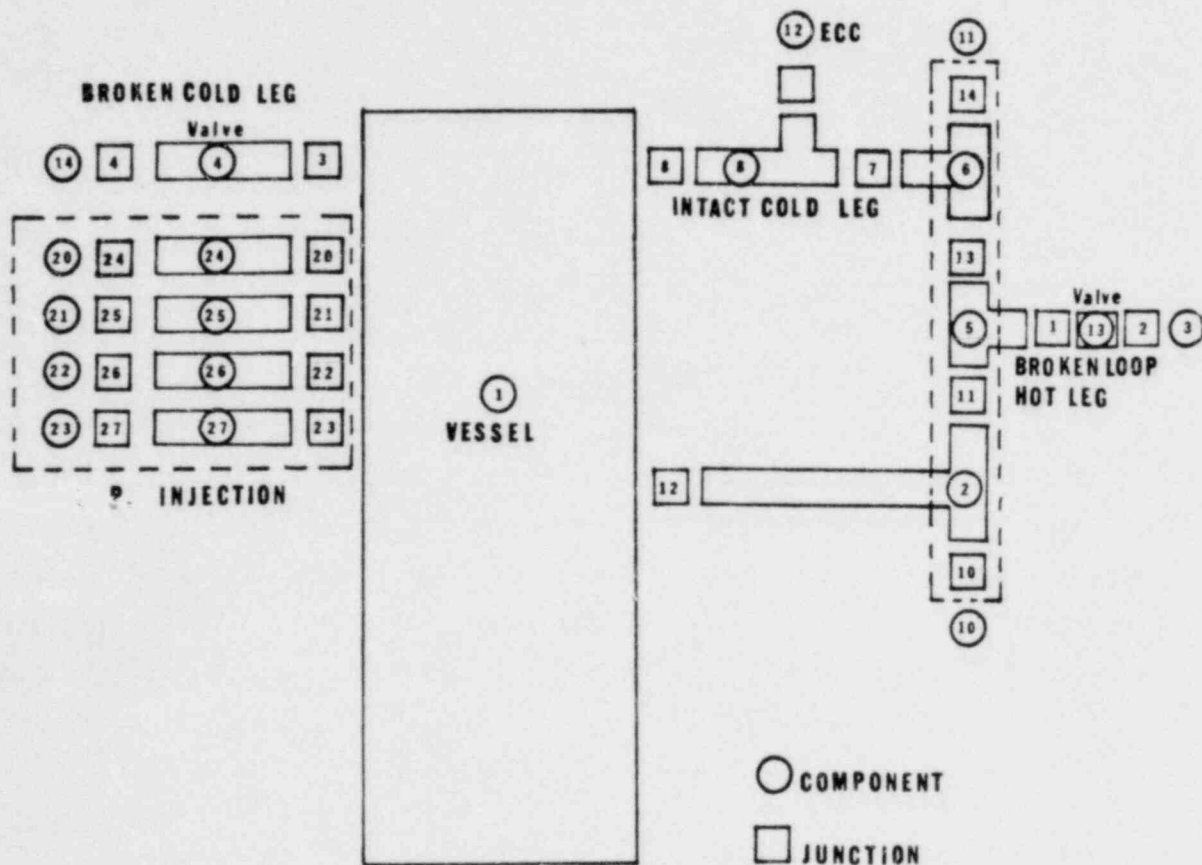


Fig. 2. SCTF system component schematic diagram.

TABLE I

ECC TEMPERATURES FOR BASIC SET OF CASES

<u>Case</u>	<u>ECC Water Temperature</u>		
	<u>Cold Leg</u>	<u>Upper Plenum</u>	<u>Extra Steam</u>
1	High	Low	Yes
2	Low	High	Yes
3	High	High	Yes
4	High	High	No
5	Low	Low	Yes

case, included for completeness. A summary of these five basic cases is given in Table I.

For these cases, "low" was defined as the GPWR reference reactor base case temperature and "high" was defined to be 100 K higher for the first three variants and 70 K higher for the rest of the variants. For this set of calculations, these temperatures corresponded to about saturation for "high" and 70-100 K subcooling for "low." Earlier reports^{5,6} have indicated that for systems with hot-leg ECC injection, the amount of water from the upper plenum penetrating through the upper core support plate (UCSP) into the core depends strongly upon the amount of subcooling present in the upper plenum. The results of this study, discussed in Sec. V, bear out this conclusion.

The parameters that were varied in the current study are depicted in Table II. These included power, axial temperature profile, tie-plate friction loss coefficients, water in the steam-water separator, and representation of the loop seal. Not all five cases were run with each variant; as it became apparent after several variants had been calculated that the macroscopic

TABLE II

VARIANTS FOR SCTF CALCULATIONS

Variant	Power	Rod	GPWR	Flow	Extra	Water in
		Temperature		Area		Steam/Water
<u>Set</u>		<u>Profile</u>	<u>ICs</u>	<u>Across</u>	<u>Steam</u>	<u>Separator</u>
				<u>UCSP</u>		
Base	11.00 MW	Flat	Old	Restrictive	Yes	No
A	6.65 MW	Flat	Old	Restrictive	Yes	No
B	6.65 MW	GPWR	Old	Restrictive	Yes	No
C	6.65 MW	Flat	Old	Unrestricted	Yes	No
D ^a	6.65 MW	GPWR	Old	Restrictive	Yes	No
E	6.65 MW	GPWR	New	Restrictive	Yes	No
F	6.65 MW	GPWR	Old	GPWR	Yes	No
G	6.65 MW	GPWR	Old	GPWR	No	No
H	6.65 MW	GPWR	Old	GPWR	No	Yes
I ^b	6.65 MW	GPWR	Old	GPWR	No	No
J ^c	6.65 MW	GPWR	Old	GPWR	No	No

^aHad additional frictional losses specified in the core.

^bIncluded updated loop-seal model.

^cRun with TRAC-PD2.

results were dominated by the ECC temperatures rather than by the other parameters, only the most promising cases (Cases 2 and 5) were run.

A considerably later version of TRAC was used for this series of calculations; it was TRAC-PIA (version 23.0) with modifications both to include additional graphics for certain integrated quantities and to correct known errors involving spurious pressure spikes and an erroneous pressure drop calculation at the core top. The only exception to this was for variant J,

which was run with the recently released TRAC-PD2 (version 26.0) completely through reflood and full quenching of the rods.

III. MODELING AND ASSUMPTIONS

All initial flow velocities are assumed to be zero. The containment is modeled as a constant pressure of 3 bars at the breaks. The steam-water separator is connected to both the hot and cold legs and is assumed to have an efficiency of 95%.

It is assumed that the entire core region of the vessel component is heated. The rods are assumed to extend to the bottom of the lower plenum. The added steam supply is assumed to be distributed uniformly across the bottom of the lower plenum for the full width of the core, injected upwards. The cold leg ECC injection enters diagonally toward the vessel. The hot-leg ECC injection is simulated by four horizontal pipes entering the upper plenum immediately above the UCSP.

The vessel representation (Fig. 1) has fourteen axial levels (five in the lower plenum, five in the core, and four in the upper plenum and upper head), eleven radial rings (one for each of the eight bundles of the core, one for the core bypass region, and two for the downcomer), and one azimuthal segment depicting the slab geometry.

The steam-water separator is modeled as a series of three tees. The central tee is connected to the valve component representing the hot leg in the broken loop, which is connected to a constant-pressure break representing the containment tank. The other two tees are connected to the vessel by means of a hot leg and an intact cold leg. The broken cold leg is represented by a valve connected to the vessel on one end and, on the other, another constant-pressure break representing the containment.

The initial vessel pressure is 6 bars; an initial temperature of 430 K was assumed for the vessel internals, the extra steam supply, the lower plenum liquid, and the primary piping. The initial rod temperatures ranged between 650 and 1067 K. The initial lower plenum liquid inventory is 56%.

A previous study² demonstrated that steam flows matching GPWR steam flows for the first few seconds of the transient could be achieved by varying valve opening times instead of opening them simultaneously at the initiation of the calculation. Hence, the hot-leg break opens linearly from $t = 0$ s over a 2-s interval, the hot-leg injection begins at $t = 0$ s, the cold-leg break opens linearly from $t = 2$ s over a 4-s interval, and the cold-leg ECC begins at $t = 2$ s. The transient time for each of the calculations was between 45 and 55 s, which was ample time to determine whether the lower plenum would refill.

IV. OVERALL SYSTEM TRANSIENT BEHAVIOR

The SCTF transient calculation begins during the end of the blowdown phase of the accident. Initial conditions for the SCTF calculation were taken from the TRAC-PIA intermediate-node GPWR calculation⁷ at the time when that system has depressurized to about 6 bars; this is at about 26 s into the GPWR transient. The intermediate-node GPWR model gives a good simulation for the refill phase of the transient. The biggest discrepancies between this and the fine-node model occur during the reflood phase, which is well past the time of interest for this study.

The hot-leg break valve begins to open and hot-leg ECC injection begins. Liquid immediately begins flowing out the hot-leg break (Fig. A-1), reaching a peak mass flow rate of 10-30 kg/s at about 5 s and in most cases dwindling to nothing by 10 s, and then trying to reenter the break at a miniscule mass flow rate for about another 10 s. By 30 s in most cases, the hot-leg break mass flow has stabilized at zero.

The cold-leg break valve begins to open at 2 s and is fully open by 6 s. There is no noticeable flow out the break until about 4 s when the cold-leg ECC injection begins. In most cases, the maximum mass flow out the cold-leg break (Fig. A-2) has been reached by about 15 s; in most cases this maximum is on the order of 300 kg/s. However, a more meaningful measure might be an average mass flow rate of 150 kg/s over a 10-s interval. By about 20 s the flow out the cold-leg break has stopped completely. This corresponds to the time when the minimum system pressure of about 2.5 bars occurs; the pressure then

oscillates near 3 bars (the containment pressure) for the rest of the transient.

The lower plenum liquid inventory (Fig. A-10) starts out at 56% and is swept out to only about 20% by 8 s; the inventory remains this low until about 20 s when refill begins. For all the cases except 2 and 5, refill never occurs during the time of the calculation (about 50 s); for simulating GPWR behavior as calculated by TRAC-PIA, refill should occur sooner than 40 s, so Cases 1, 3, and 4 are considered unacceptable. For the acceptable cases, however, the lower plenum was completely filled by 30-35 s and remains full except for small depletions on the order of a few percent.

The core inlet liquid and vapor mass flow rates (Figs. A-5 and A-6) are initially small but oscillatory because of small localized pressure bursts caused by the vaporizing of entrained liquid droplets until the lower plenum has refilled; then the liquid entering the hot core from the full lower plenum vaporizes with greater pressure bursts. At this point, TRAC-PIA had difficulty in handling the heat transfer from the rods to the liquid, and the calculation was stopped for all the variations except J, which was run with TRAC-PD2 and had the advantage of its greatly improved heat transfer solution scheme. Variation J was calculated through full core quenching and reflood and is discussed in detail in another report.⁸

The core outlet liquid and vapor mass flow rates are shown in Figs. A-7 and A-8. These illustrate that the steam flow from the core is upward, and that when it is relatively small, there is a fair amount of liquid fallback from the upper plenum into the core. In addition, a small amount of liquid enters the upper plenum from the core, entrained by the steam flow.

At the start of the transient, the core is devoid of liquid (Fig. A-9); gradually its liquid inventory increases in an oscillatory manner to a maximum of 25%. This liquid comes mainly from the fallback from the upper plenum, with a small amount coming from the lower plenum as entrained droplets.

The upper plenum initially is virtually empty (Fig. A-14), but because the hot-leg ECC is turned on immediately, it begins to fill. Case 2 was, in general, able to accumulate a liquid pool of about 40% above the upper core support plate, but Case 5 consistently filled to over 80%. Figure A-15, average upper plenum liquid temperature, shows that Case 5 is more subcooled than Case 2, so this result is anticipated. Figures A-16 and A-17, upper plenum average saturation temperature and average pressure, are included for completeness.

As a result of the larger upper plenum pool formation and greater liquid fallback, the rod temperatures (Fig. A-18) were consistently lower for Case 5, with the temperature reversal occurring at about 30 s.

For Case 5J, the case run out through full reflood with TRAC-PD2, the timing of events was somewhat different, but the overall behavior of this early portion of the transient was the same. This calculation is described fully in another report.⁸

V. RESULTS OF THE STUDY

The only one of the prescribed four cases to refill the lower plenum consistently is Case 2, the one with the subcooled cold-leg and near-saturated upper plenum ECC injection temperatures. However, Case 5 (with subcooled liquid in both injection modes) not only consistently fills the lower plenum but also results in more typical cooling of the rods during this early part of the transient.

Graphics for the following parameters for selected cases and variations appear in Appendix A:

Hot- and cold-leg break mass flow rates;

Vessel inlet and outlet mass flow rates;

Upper and lower plenum liquid volume fraction, average pressure, average liquid temperature, and average saturation temperature;

Core liquid volume fraction;

Core inlet and outlet vapor and liquid mass flow rates; and

Maximum average cladding temperatures.

Because an excessively restrictive flow area was used for the upper core support plate for Variations A through E (with the exception of Variation C, which had no restriction at all), only Variations F through J are totally applicable to the study with respect to the GPWR. These variations all had the proper GPWR end-box flow areas used for the upper core support plate.

Both Cases 2 and 5, with their three variations F through H, agree well with the GPWR in lower plenum liquid volume fraction, average pressure, average liquid temperature, and average saturation temperature (see Figs. A-10 through A-13). Case 5F shows more core inlet vapor flow (Fig. A-6) than the others because it has the extra steam injection. Case 5 gives greater pool formation in the upper plenum (Fig. A-14), but also allows more liquid to drain into the core (Fig. A-9), accounting in part for the improved core thermal response (Fig. A-18). Case 5 gives better agreement with the GPWR in vessel inlet mass flow (Fig. A-3), but Case 2 agrees better in vessel outlet mass flow (Fig. A-4).

Of the variations F and beyond, Variation G with no extra steam does as well or better than the variation with steam, F. Variation H, with water in the steam-water separator, has little if any effect in changing the results of Variation G. Variation I, with the most exact representation of the loop seal, again has little effect in changing the result of G.

Variation J, which differed from Variation I only in the use of TRAC-PD2 instead of TRAC-PlA, showed the same overall behavior for the initial refill period except that the time scale was somewhat lengthened. However, the most recent fine-node German PWR calculation (August 1980), also run with TRAC-PD2, showed about the same temporal behavior in both refill and reflood as Variation J.

The only case run with Variations I and J was what appeared to be the most promising: Case 5. Because the previous calculations indicated that in general Case 5 produced more reasonable results than all the others except Case 2, all the other variations were not calculated past lower plenum refill (for those cases in which this occurred in a time comparable to GPWR refill time).

VI. CONCLUSIONS

The consistent filling of the lower plenum in Case 2 throughout the first nine variations,* and in Case 5 throughout the last five variations,** is a strong indicator that reasonably typical refill behavior can be achieved when subcooled ECC water (on the order of 70-100 K subcooling) is injected into the cold leg. Further, by injecting subcooled water into the upper plenum as well as into the cold leg, even better agreement with the German reference reactor can be attained.

In addition, it would seem that the added complexity of extra steam injection for all the tests could unnecessarily complicate the interpretation of the experimental results. Therefore, to the extent investigated in this study, extra steam injection into the vessel does not appear to be warranted for combined injection refill/reflood tests.

*This case was run only through Variation H.

**This case was run only for Variation F and Beyond.

REFERENCES

1. "TRAC-PIA: An Advanced, Best-Estimate Computer Program for PWR LOCA Analysis," Los Alamos National Laboratory report LA-7777-MS, NUREG/CR-0665 (May 1979).
2. D. Dobranich, S. T. Smith, J. R. Ireland, and P. B. Bleiweis, "SCTF Combined Injection Steam Supply Studies," in Nuclear Reactor Safety Quarterly Progress Report for January 1 - March 31, 1979, J. F. Jackson, M. G. Stevenson, Comp., Los Alamos National Laboratory report LA-7867-PR, NUREG/CR-0868 (June 1979).
3. S. T. Smith, "SCTF Steam Supply Study," in Nuclear Reactor Safety Quarterly Progress Report for April 1 - June 30, 1979, J. F. Jackson, M. G. Stevenson, Comp., Los Alamos National Laboratory report LA-7968-PR, NUREG/CR-0993 (August 1979).
4. S. T. Smith, "SCTF Steam Supply Studies," in Nuclear Reactor Safety Quarterly Progress Report for January 1 - March 31, 1980, M. G. Stevenson, J. F. Jackson, and J. C. Vigil, Comp., Los Alamos National Laboratory report LA-8494-PR, NUREG/CR-1694 (August 1980).
5. C. J. Crowley, J. A. Black, and C. N. Carey, "Downcomer Effects in a 1/15-Scale PWR Geometry - Experimental Data Report," NUREG-028 (May 1977).
6. CCFL/Reflood System Effects Task Plan Document - to be published by General Electric Nuclear Energy Engineering Division.
7. D. Dobranich, "German Reference Reactor Calculations," in Nuclear Reactor Safety Quarterly Progress Report for January 1 - March 31, 1980, M. G. Stevenson, J. F. Jackson, and J. C. Vigil, Comp., Los Alamos National Laboratory Report LA-8494-PR, NUREG/CR-1694 (August 1980).
8. S. T. Smith, "Comparison of the TRAC Computational Results for the Siao Core Test Facility Model and the Reference German PWR During Reflood," Los Alamos National Laboratory report LA-8704-MS (in press).

APPENDIX

GRAPHICS FOR SELECTED PARAMETERS, VARIANTS, AND CASES

- A-1. Hot-leg break mass flow rate.
- A-2. Cold-leg break mass flow rate.
- A-3. Vessel inlet mass flow rate.
- A-4. Vessel outlet mass flow rate.
- A-5. Core inlet liquid mass flow rate.
- A-6. Core inlet vapor mass flow rate.
- A-7. Core outlet liquid mass flow rate.
- A-8. Core outlet vapor mass flow rate.
- A-9. Core liquid volume fraction.
- A-10. Lower plenum liquid volume fraction.
- A-11. Lower plenum average liquid temperature.
- A-12. Lower plenum average saturation temperature.
- A-13. Lower plenum average pressure.
- A-14. Upper plenum liquid volume fraction.
- A-15. Upper plenum average liquid temperature.
- A-16. Upper plenum average saturation temperature.
- A-17. Upper plenum average pressure.
- A-18. Average cladding temperature.

HOT-LEG BREAK MASS FLOW RATE

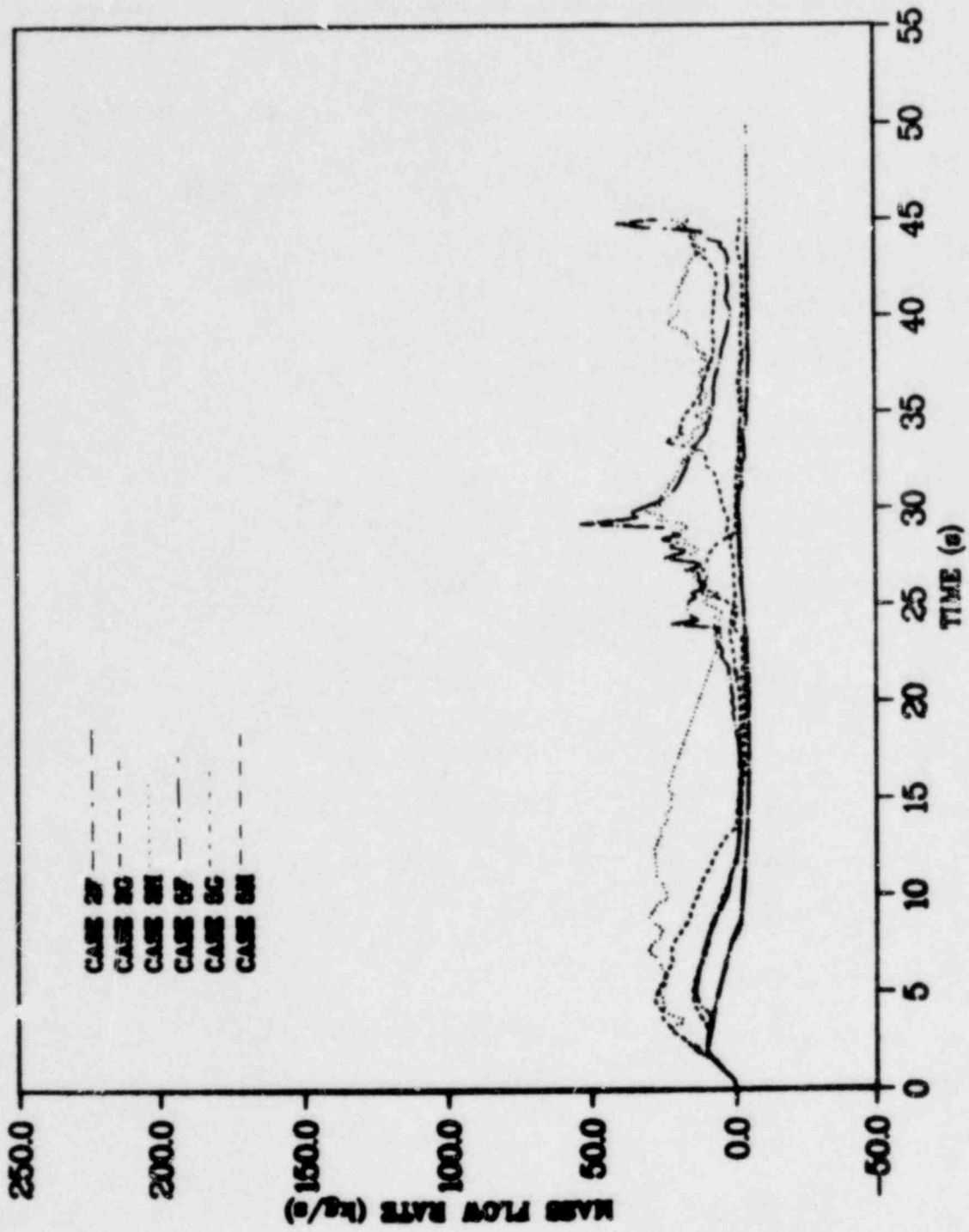


Fig. A-1. Hot-leg break mass flow rate.

COLD-LEG BREAK MASS FLOW RATE

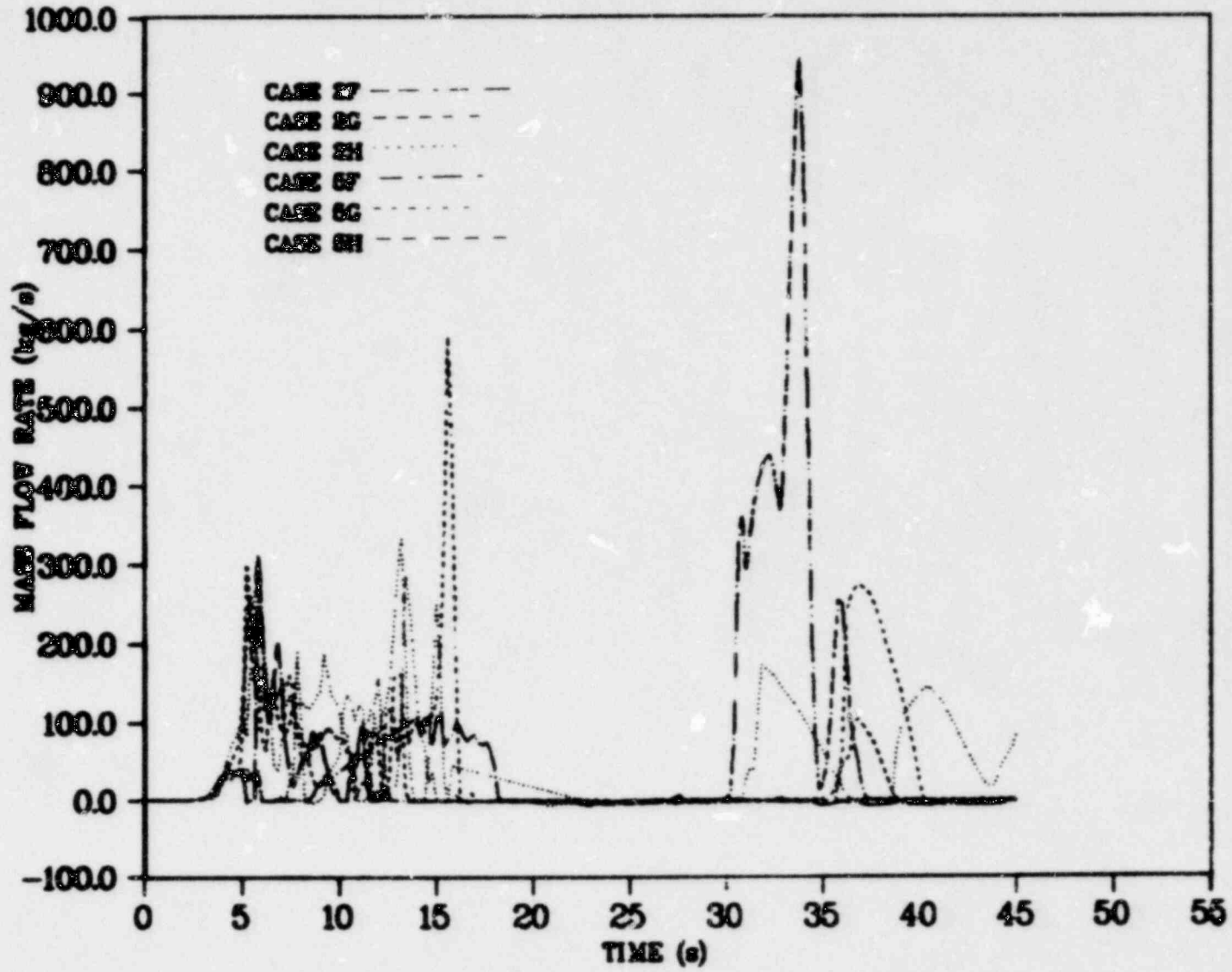


Fig. A-2. Cold-leg break mass flow rate.

INTACT COLD-LEG ENTRANCE MASS FLOW RATE

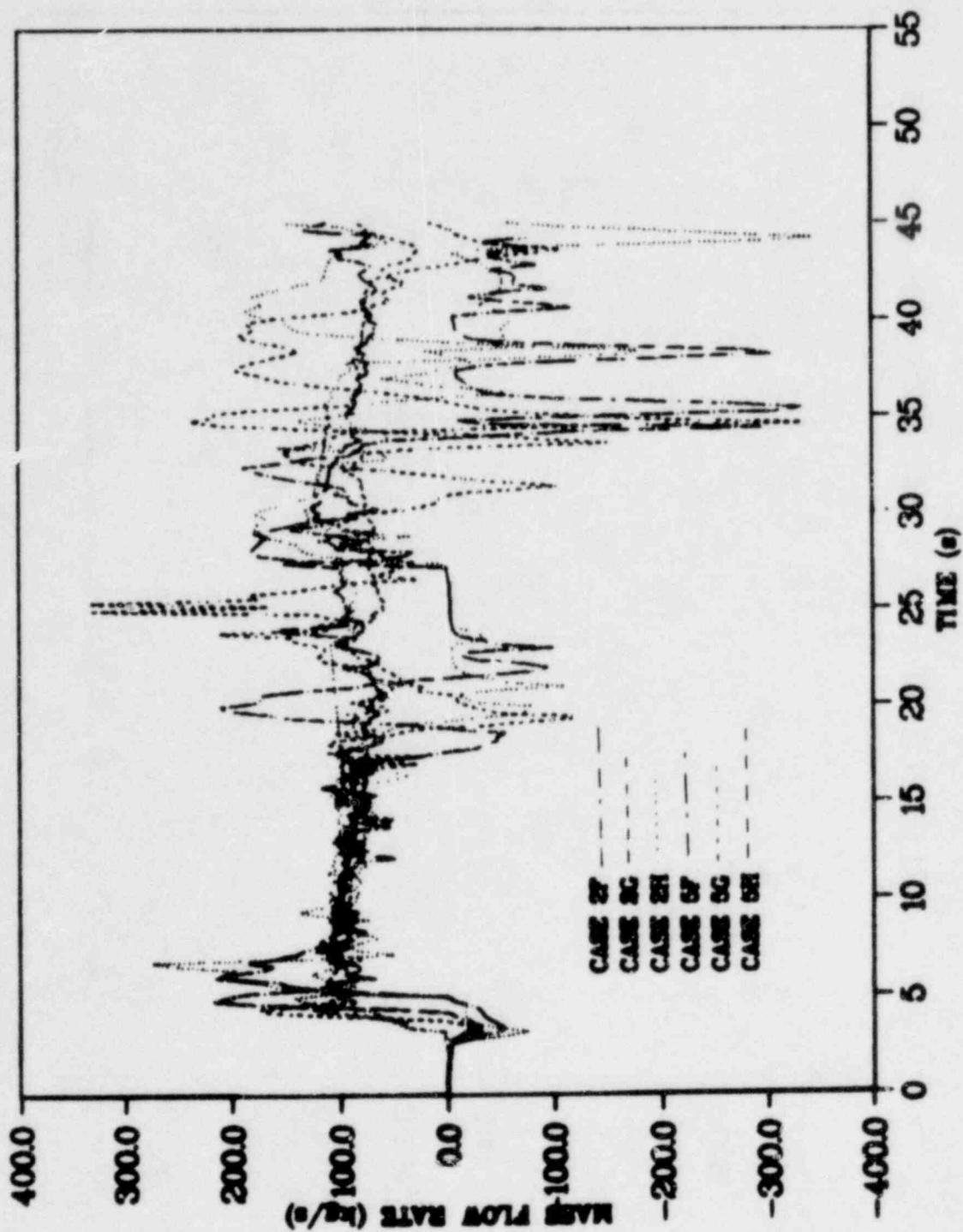


Fig. A-3. Vessel inlet mass flow rate.

HOT-LEG EXIT MASS FLOW RATE

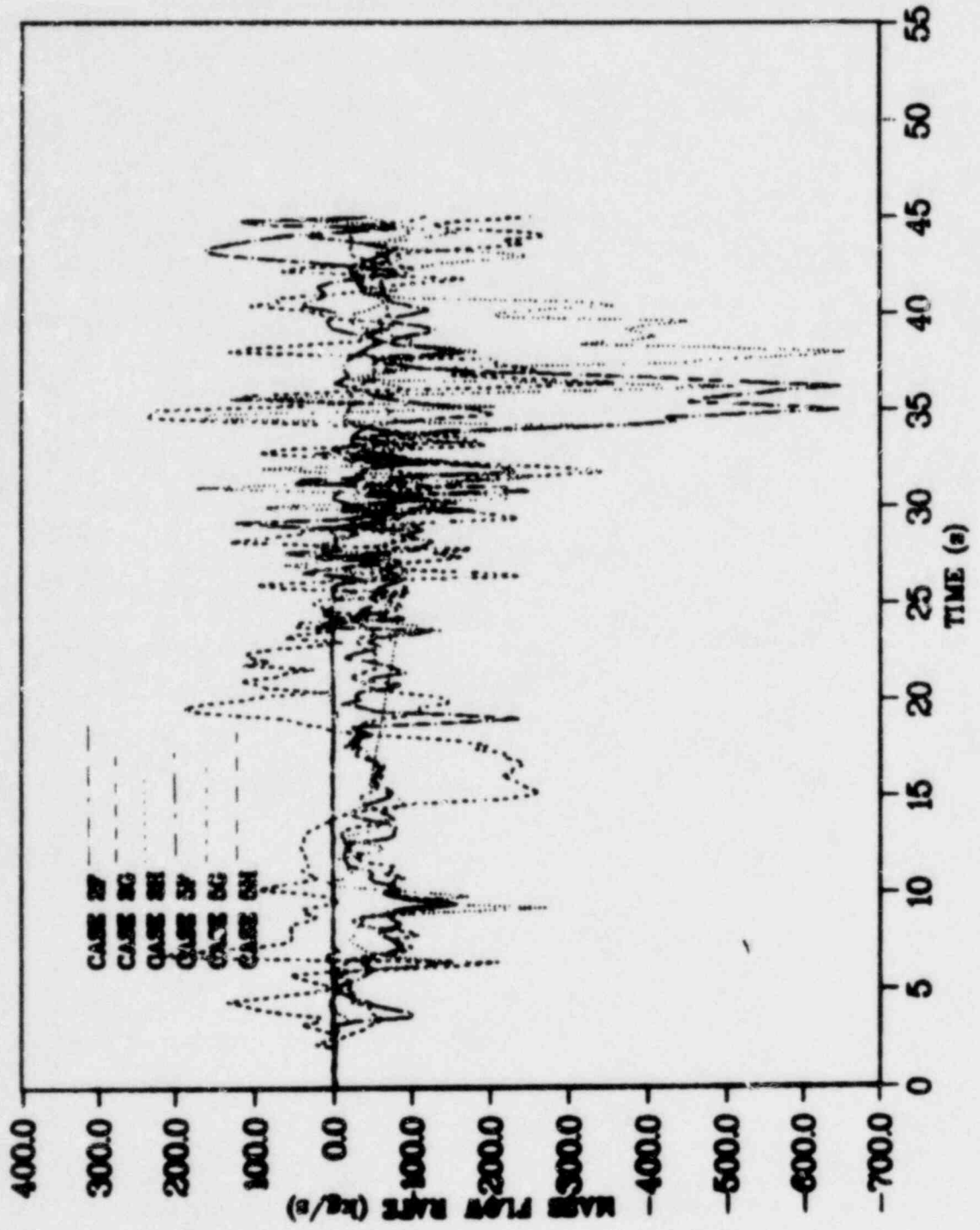


Fig. A-4. Vessel outlet mass flow rate.

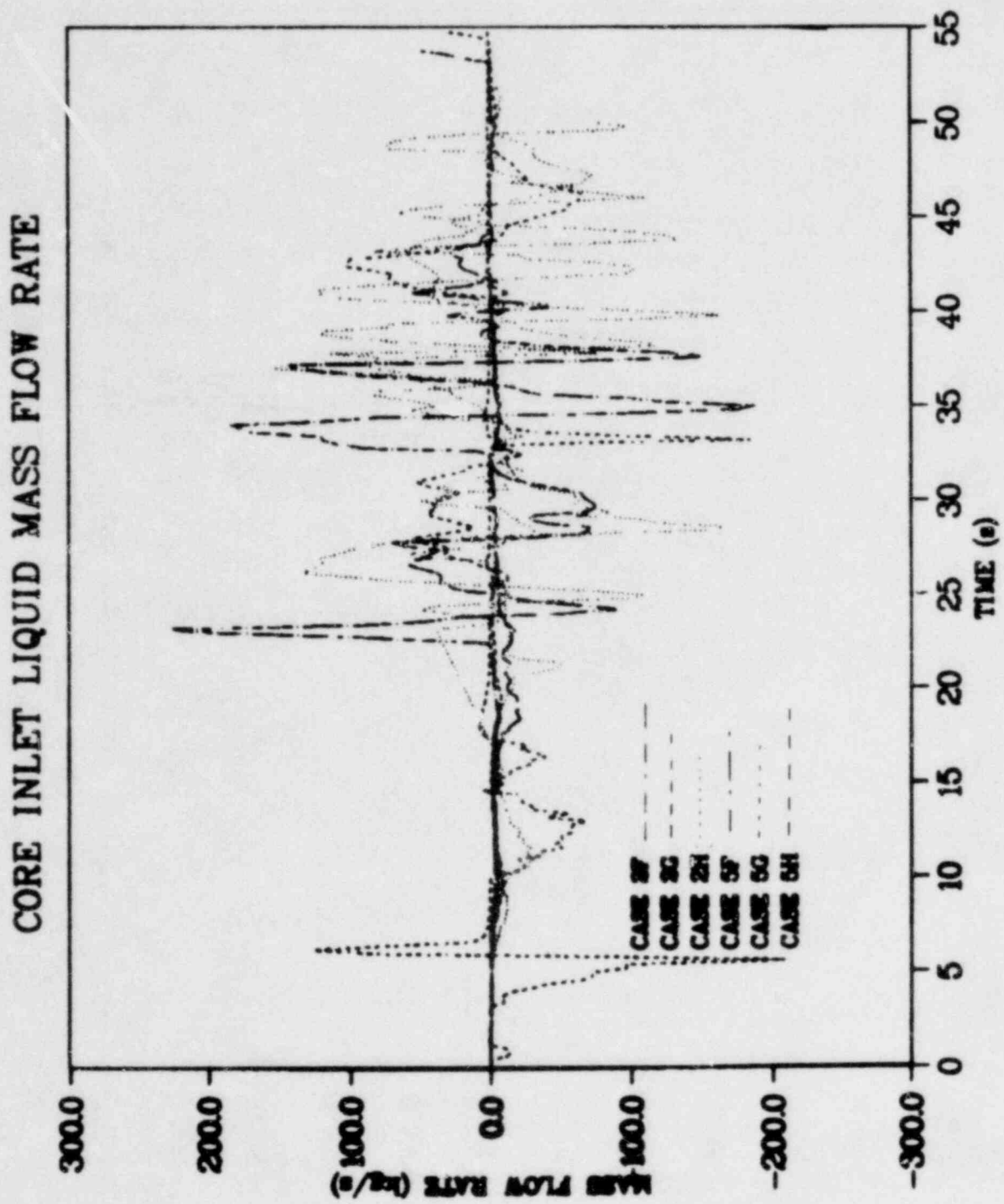


Fig. A-5. Core inlet liquid mass flow rate.

CORE INLET VAPOR MASS FLOW RATE

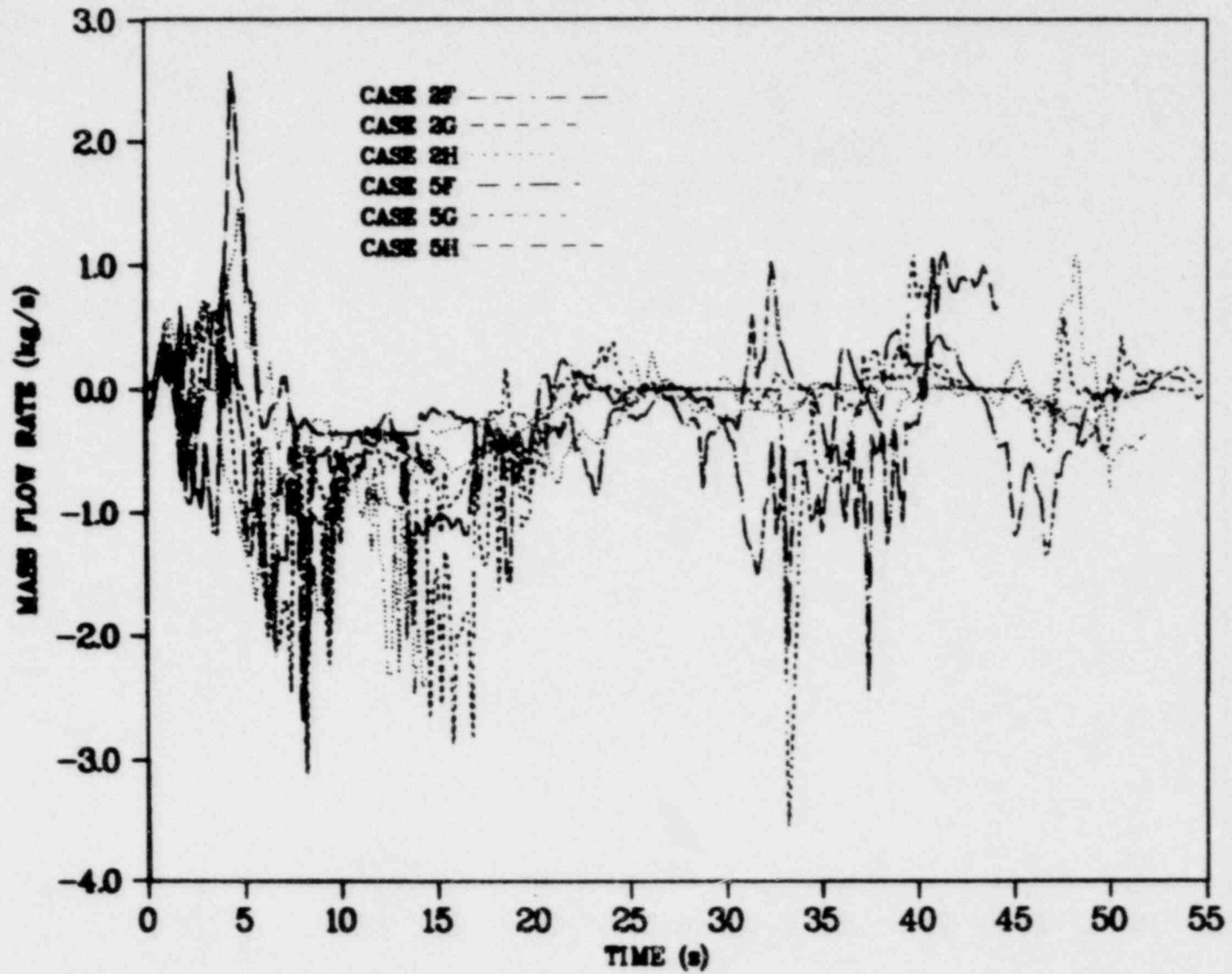


Fig. A-6. Core inlet vapor mass flow rate.

CORE OUTLET LIQUID MASS FLOW RATE

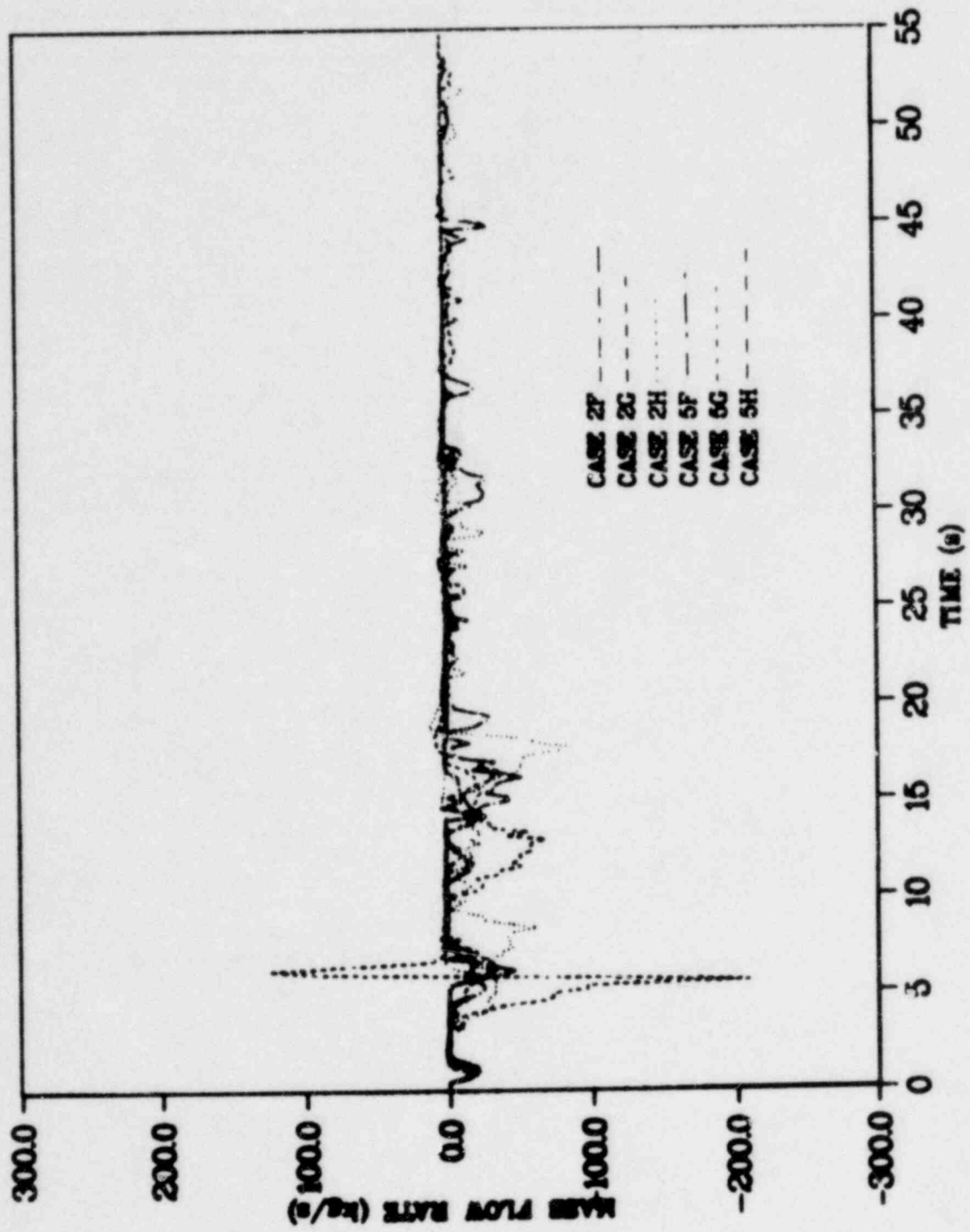


Fig. A-7. Core outlet liquid mass flow rate.

CORE OUTLET VAPOR MASS FLOW RATE

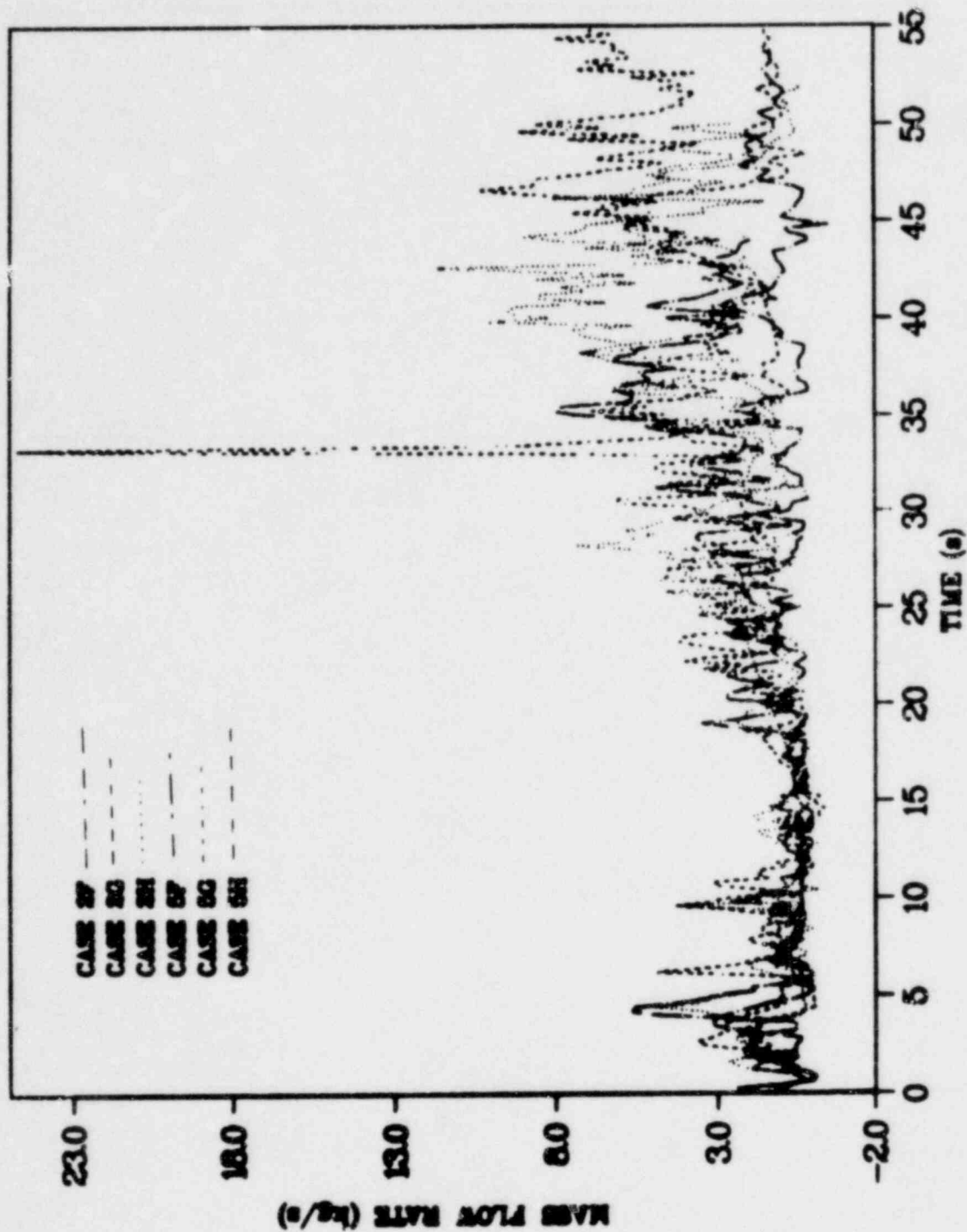


Fig. A-8. Core outlet vapor mass flow rate.

CORE LIQUID VOLUME FRACTION

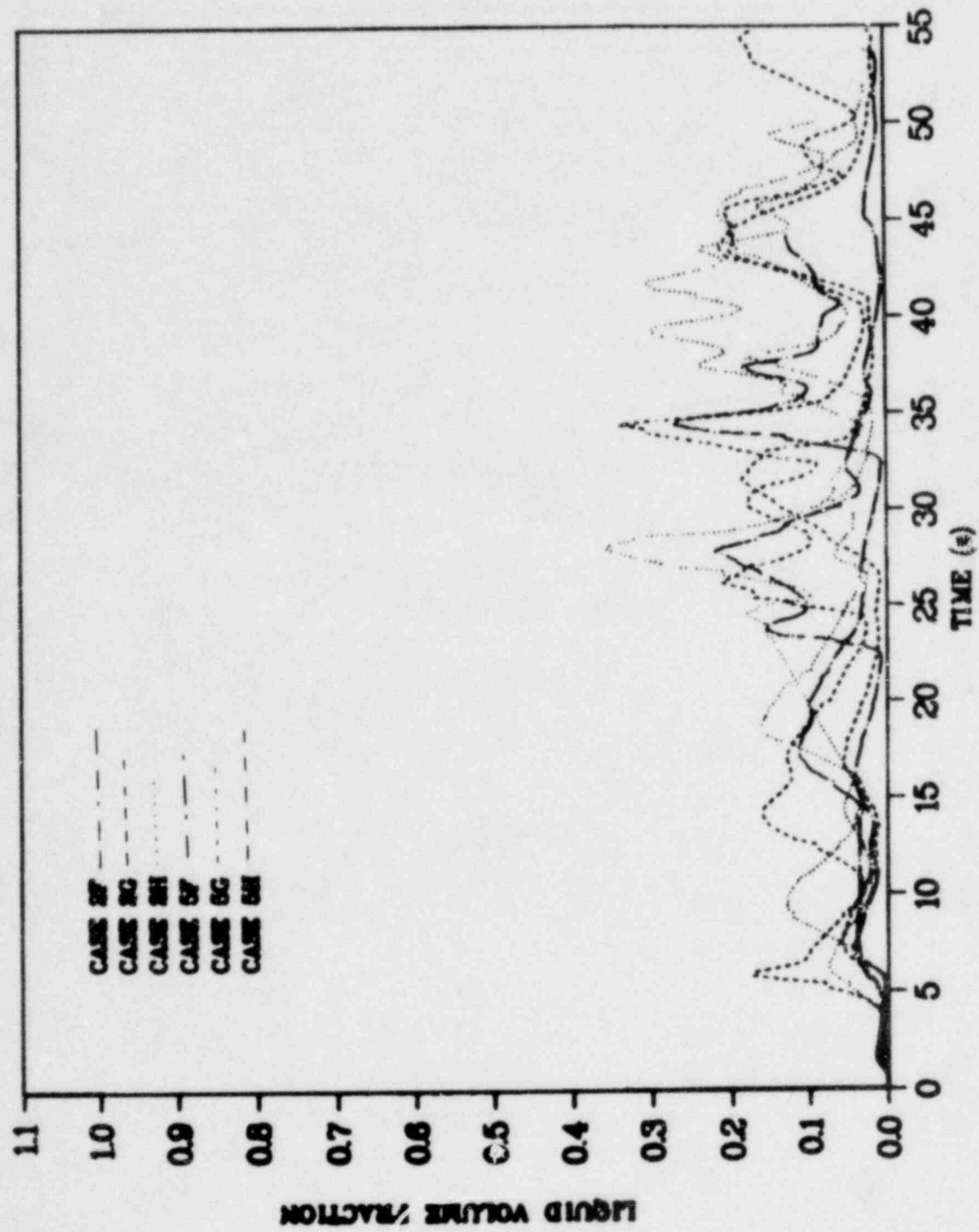


Fig. A-9. Core liquid volume fraction.

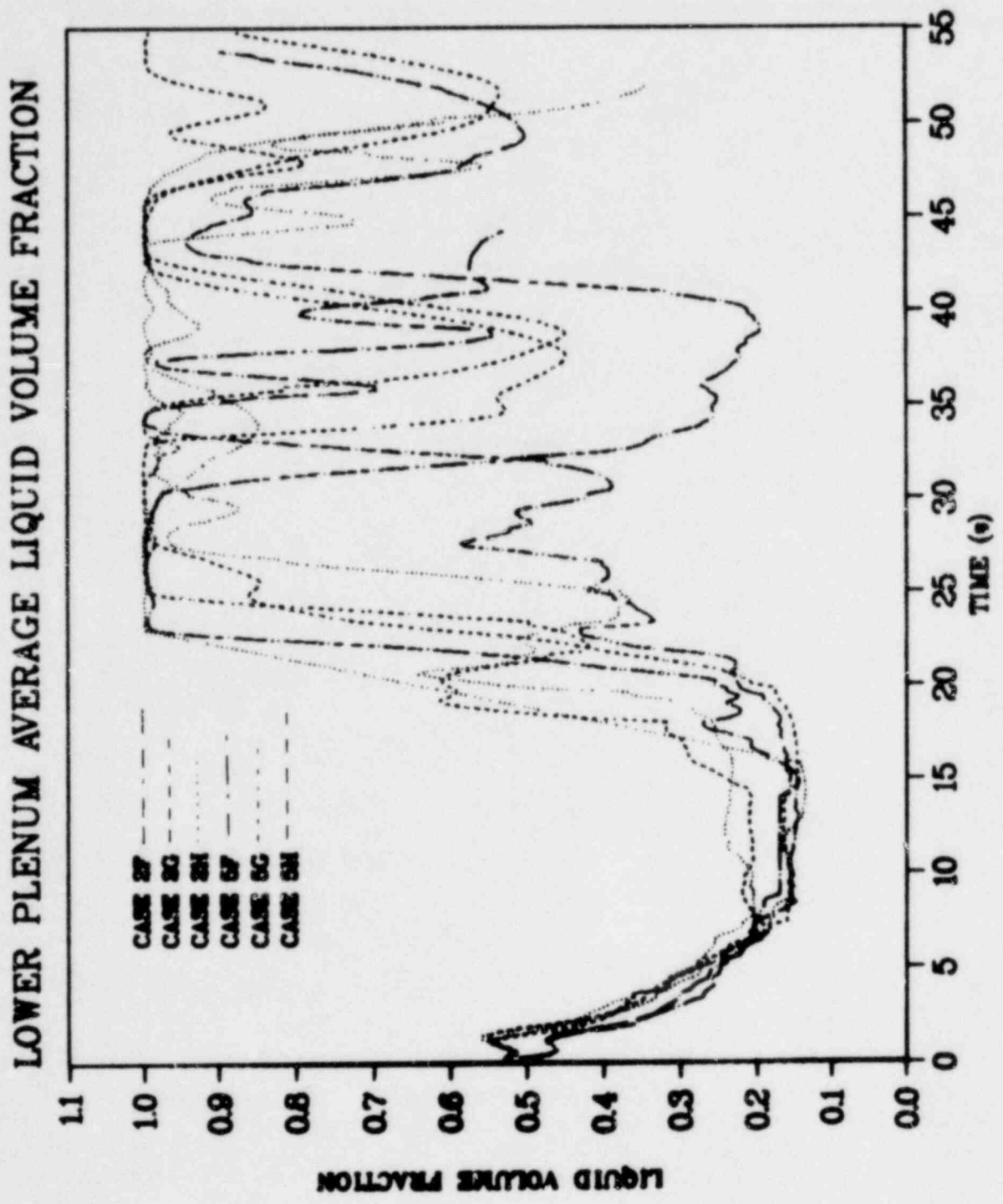


Fig. A-10. Lower plenum liquid volume fraction.

LOWER PLENUM AVERAGE LIQUID TEMPERATURE

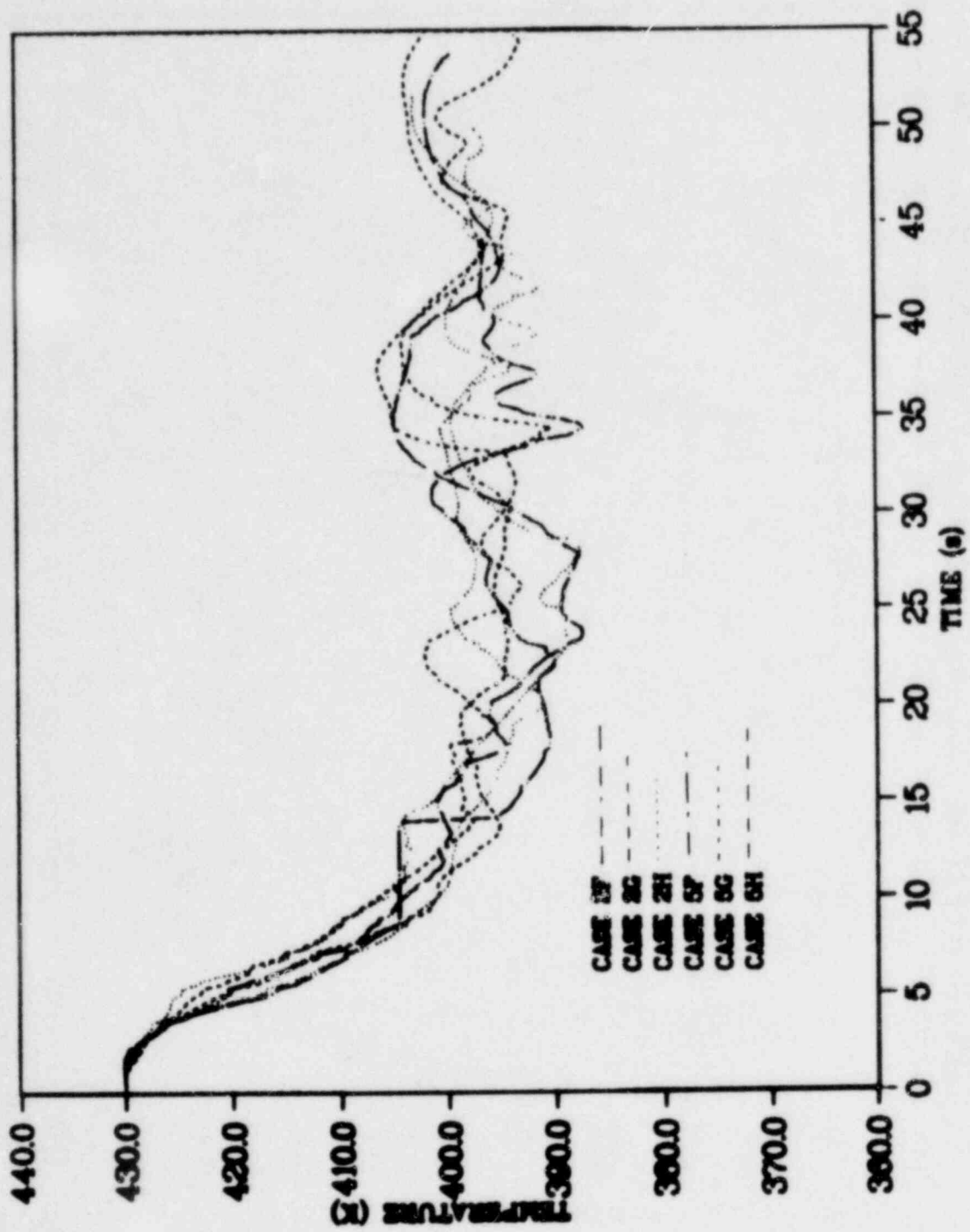


Fig. A-11. Lower plenum average liquid temperature.

LOWER PLENUM AVERAGE SATURATION TEMPERATURE

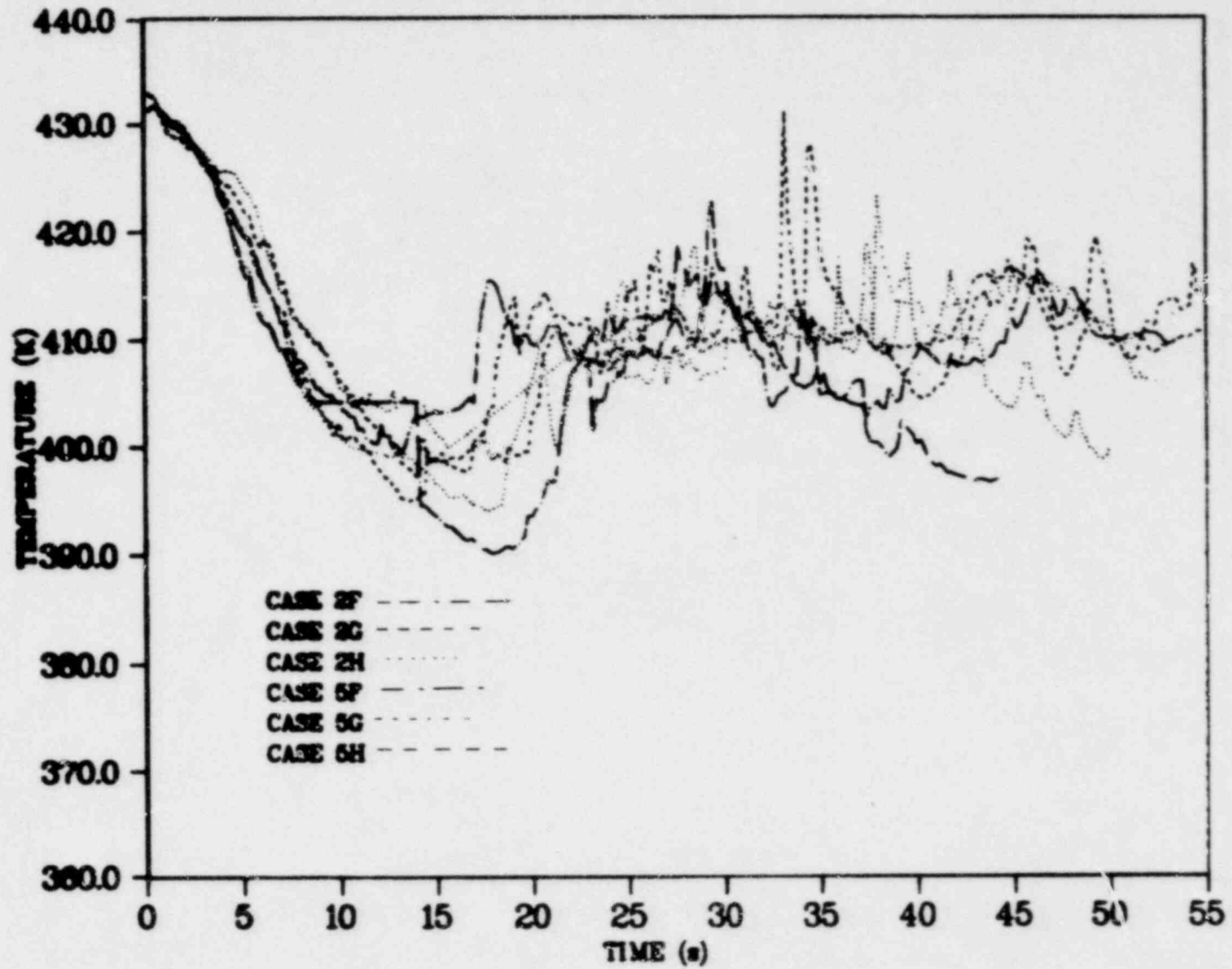


Fig. A-12. Lower plenum average saturation temperature.

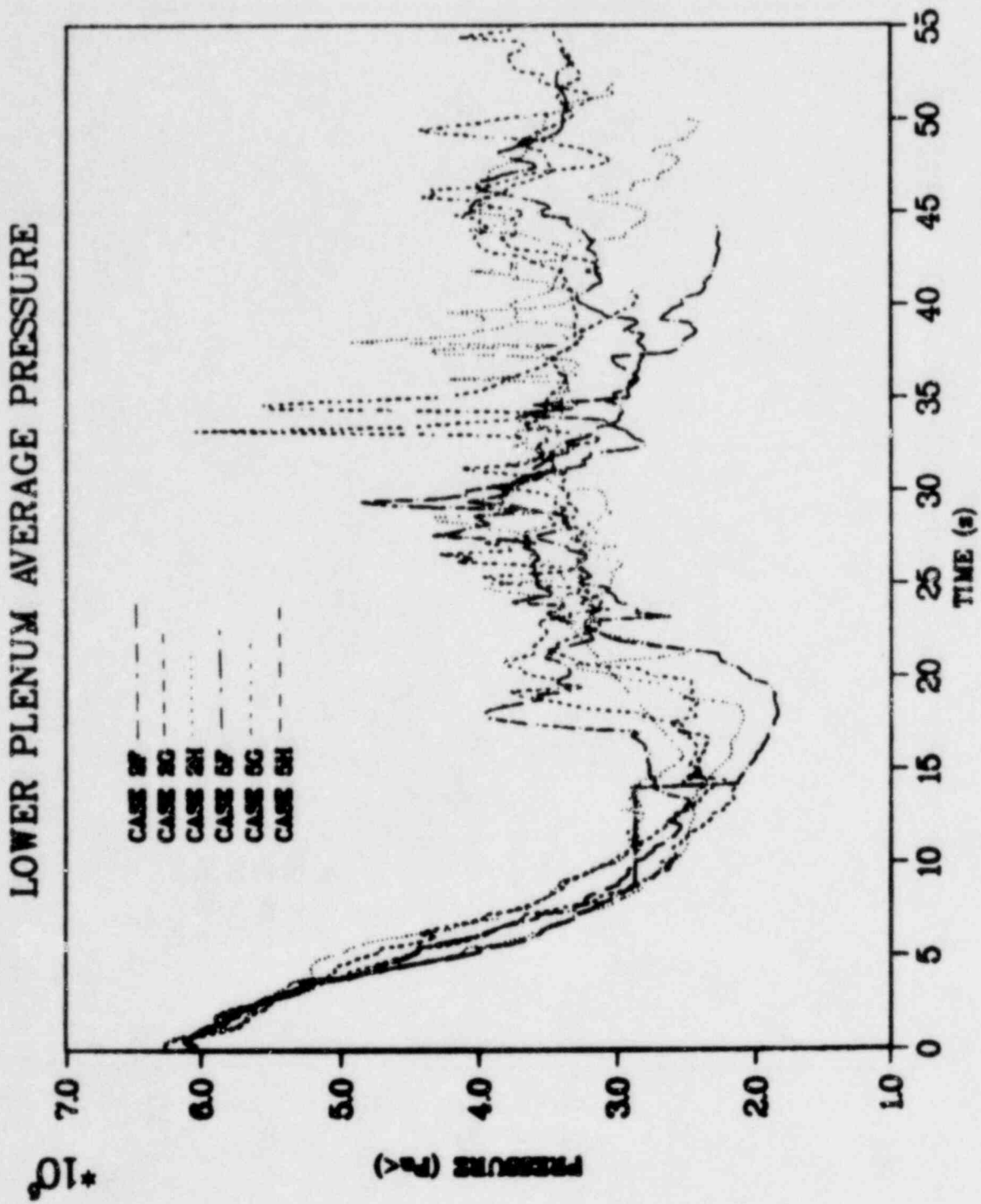


Fig. A-13. Lower plenum average pressure.

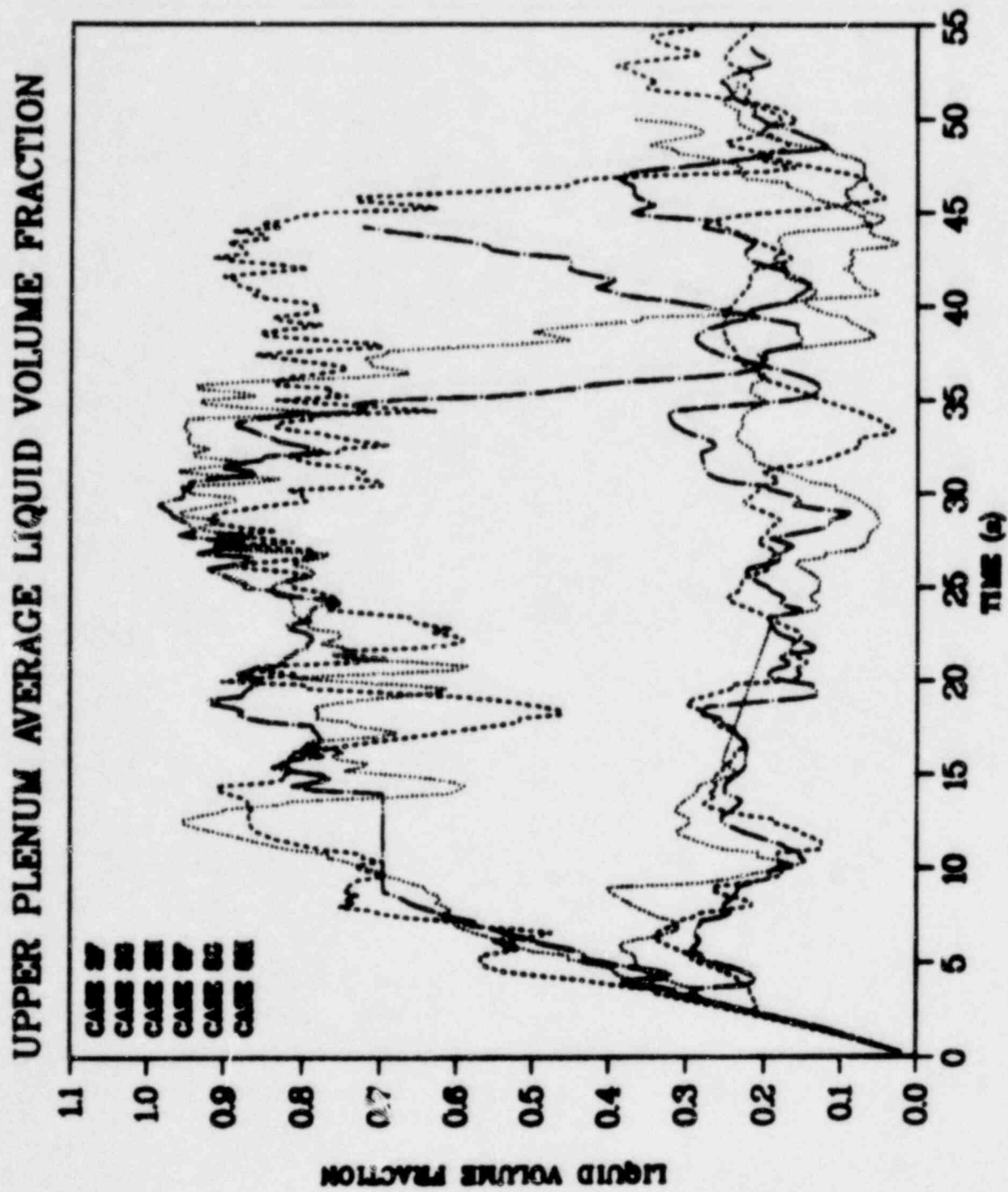


Fig. A-14. Upper plenum liquid volume fraction.

UPPER PLENUM AVERAGE LIQUID TEMPERATURE

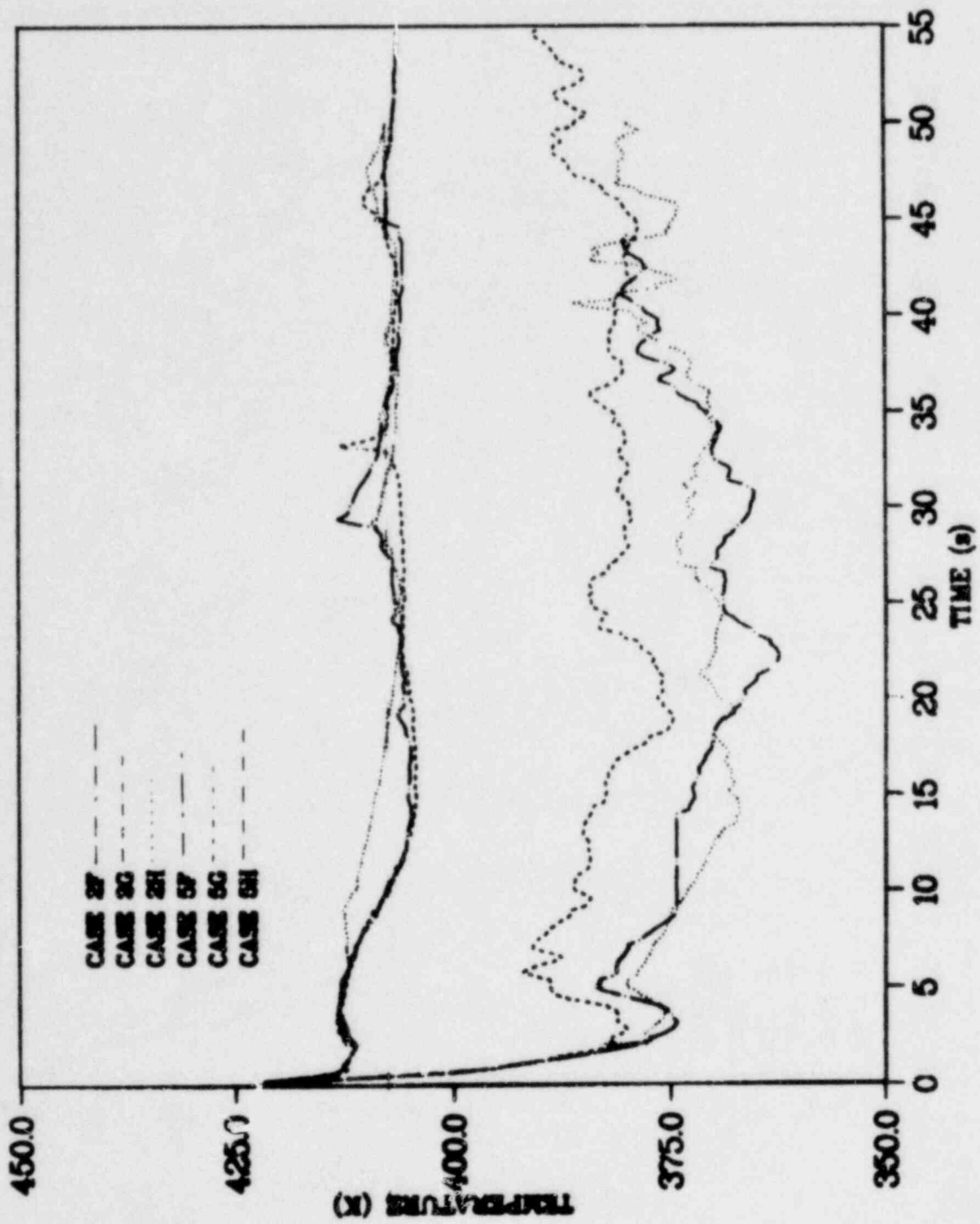


Fig. A-15. Upper plenum average liquid temperature.

UPPER PLENUM AVERAGE SATURATION TEMPERATURE

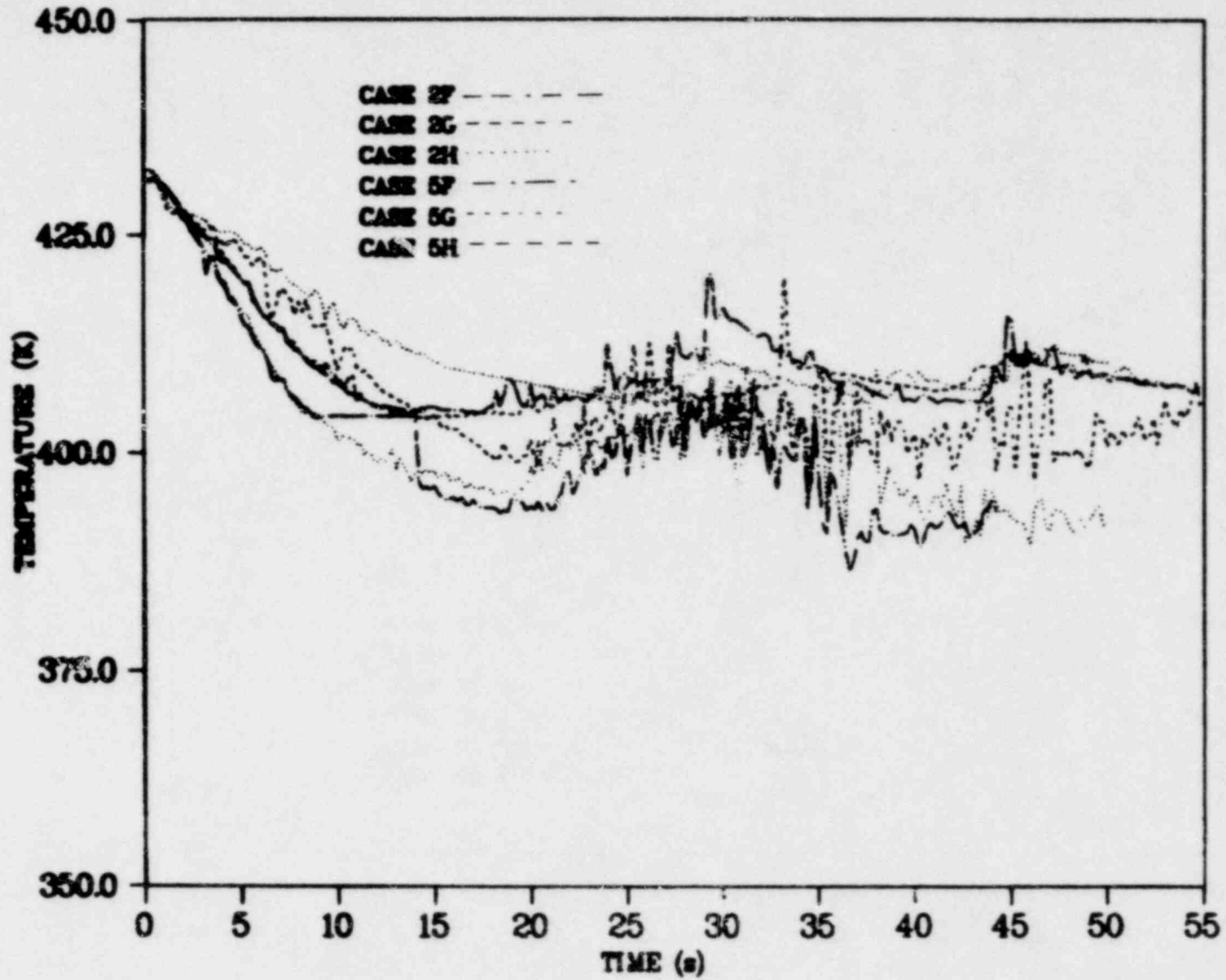


Fig. A-16. Upper plenum average saturation temperature.

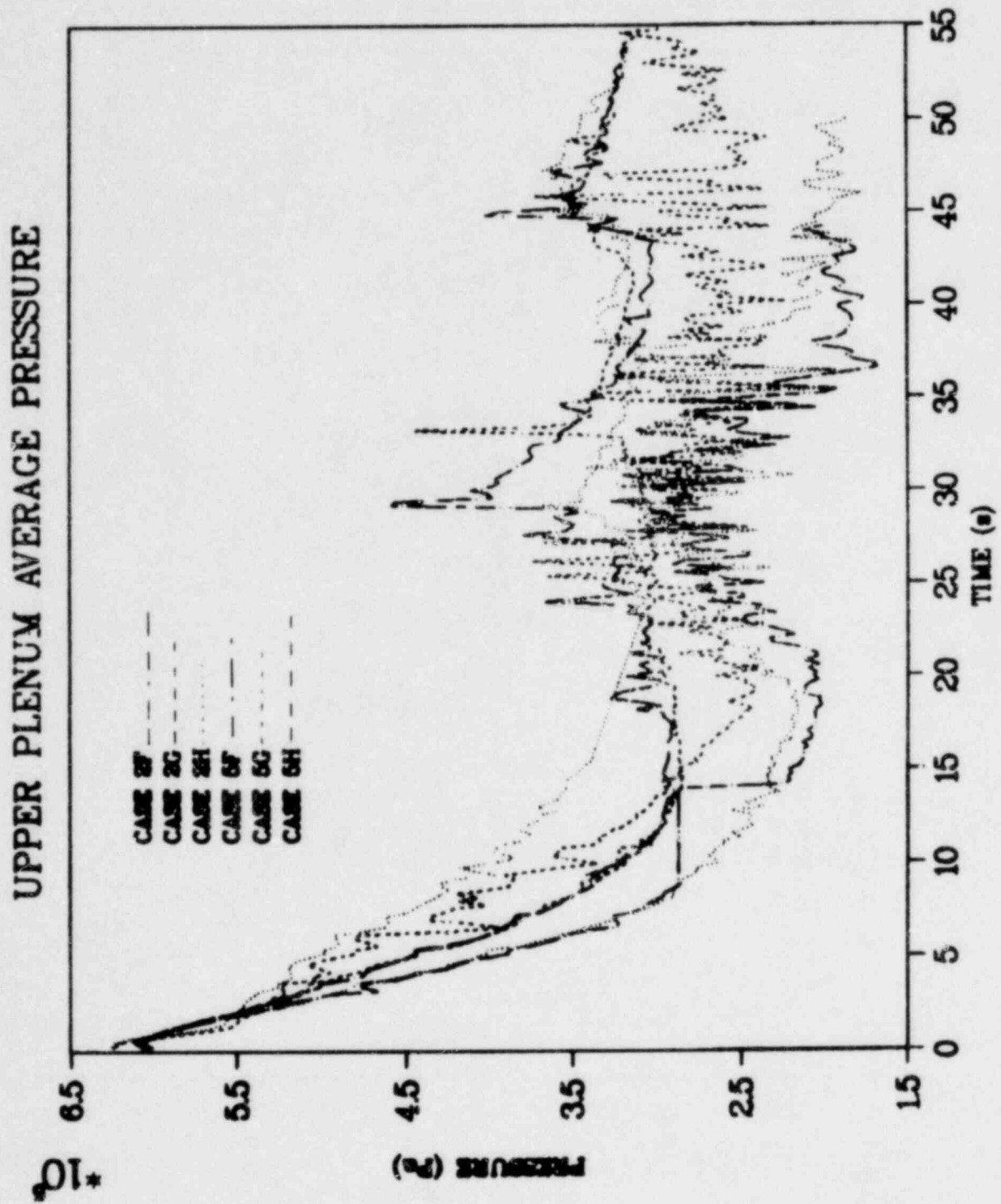


Fig. A-17. Upper plenum average pressure.

MAXIMUM AVERAGE ROD TEMPERATURE

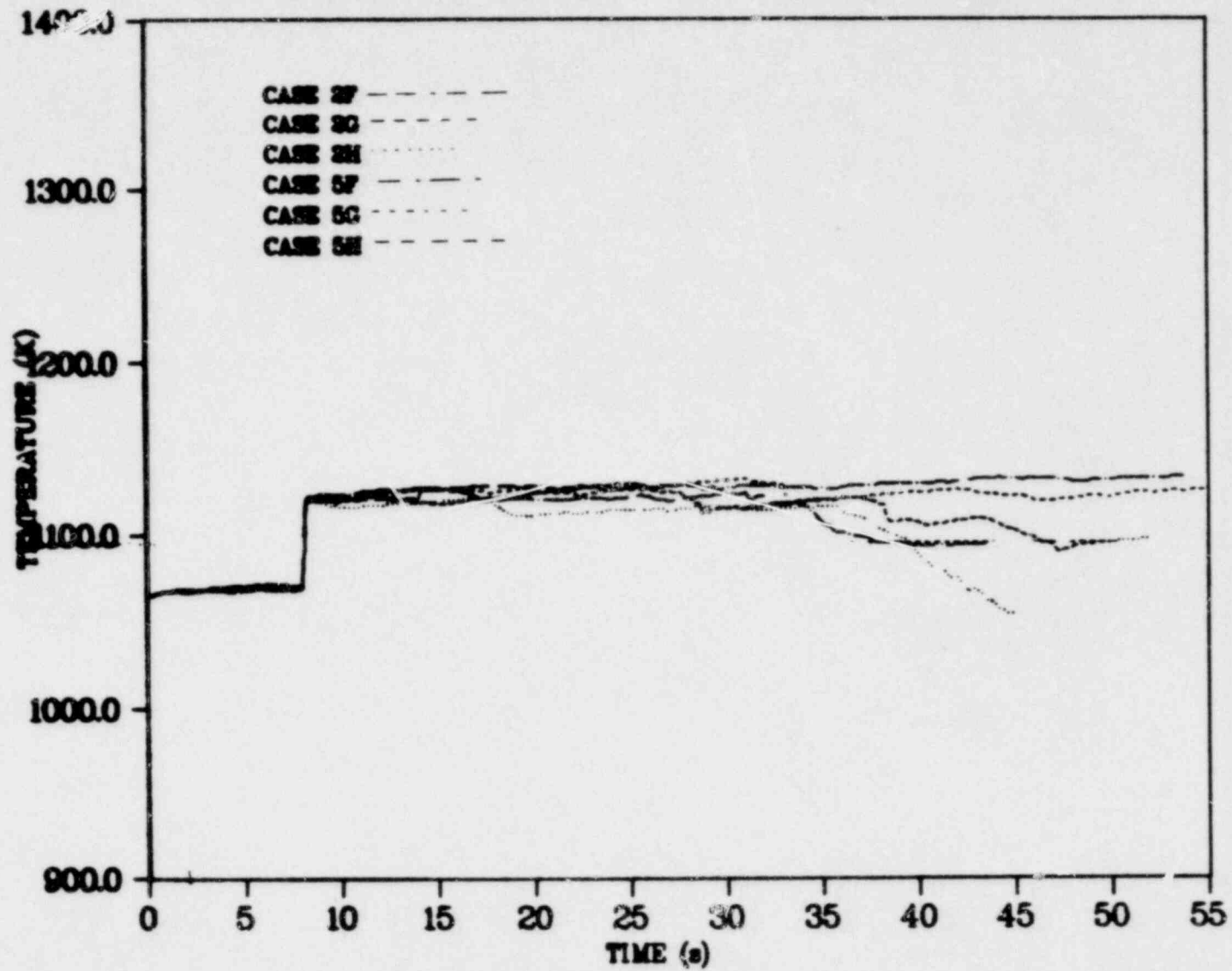


Fig. A-18. Average cladding temperature.

DISTRIBUTION

	<u>Copies</u>
Nuclear Regulatory Commission, R4, Bethesda, Maryland	388
Technical Information Center, Oak Ridge, Tennessee	2
Los Alamos National Laboratory, Los Alamos, New Mexico	<u>50</u>
	440

Available from
GPO Sales Program
Division of Technical Information and Document Control
US Nuclear Regulatory Commission
Washington, DC 20555
and
National Technical Information Service
Springfield, VA 22161